

Properties of Zinc alloy electrodeposits produced from acid and alkaline electrolytes

Chandrasekar M. S. · Shanmugasigamani Srinivasan ·
Malathy Pushpavanam

Received: 26 December 2007 / Revised: 1 April 2008 / Accepted: 29 May 2008 / Published online: 11 July 2008
© Springer-Verlag 2008

Abstract Zinc–cobalt (Zn–Co) and zinc–nickel (Zn–Ni) alloy electrodeposits each prepared from acid and alkaline formulations were compared for their properties. Compared to alkaline baths, acid baths offer higher metal percent of the alloying element and higher current efficiency. In alkaline baths, the variation of metal percent in deposit with current density is less significant, but that of current efficiency with current density is more. Electrolyte pH does not change significantly in alkaline solutions compared to acid solutions. X-ray diffraction evaluation of Zn–Co deposits from both electrolytes indicated their presence in the η -phase, while Zn–Ni shows pure γ -phase for deposits obtained from alkaline solutions and the existence of γ -phase with traces of η -phase of zinc for deposits obtained from the acid electrolytes. Scanning electron microscope examination shows finer grain structure for deposits obtained from alkaline solutions, and atomic force microscope studies confirm their nanostructure with reduced surface roughness. Deposits obtained from the alkaline baths exhibited higher corrosion resistance probably due to their nanostructure.

Keywords Electrodeposited zinc alloys · Comparison of baths · Cathodic current efficiency · Morphology · Corrosion resistance

Introduction

The application of sacrificial coatings onto steel and other ferrous substrates has long been established as an effective and

reliable standard of the industry for corrosion protection. Recent demands for higher quality and longer lasting finishes have prompted a move to alloy zinc deposits especially in the automotive industry, aerospace, fastener and electrical component fields [1–4]. Additionally, cadmium plating is being replaced by zinc alloy plating due to its toxic nature [5–9].

Several zinc alloy systems have been introduced, giving deposits of varied properties [6, 10]. The differences come not only from the choice of alloying metal but from the electrolyte used as well. The alloying elements successfully used with zinc are iron, cobalt, nickel and tin. The fundamental function of iron, cobalt and nickel in the zinc alloy is to modify the corrosion potential of the deposit. The alloy becomes slightly nobler than zinc, and hence, the corrosion rate of the alloy is slowed. At the same time, the deposit is still sacrificial with respect to steel. Consequently, the same thickness of an alloy has the ability to protect the underlying steel for a longer time than conventional zinc [11–18].

In response for better corrosion protection, both acid and alkaline processes have been developed [19–25]. As with the conventional zinc, both formulations have advantages and disadvantages. In general, the acid bath exhibits higher cathode current efficiency (CCE) but has poor deposit distribution on the substrate [26]. This has the added advantage of being able to plate over hardened steel and cast iron. Alkaline processes tend to have lower CCE but exhibit very good plate distribution and contain complexes that affect waste treatment. The desired cobalt content in the alloy to achieve the above advantages is only 0.6–0.8% compared with the zinc–nickel alloy requiring ~14% and 10–12% nickel when plated from acid and alkaline solutions, respectively [27, 28].

This paper compares the properties of zinc–nickel (Zn–Ni) and zinc–cobalt (Zn–Co) alloy deposits each obtained from an acid sulfate and sodium hydroxide electrolytes.

C. M. S. · S. Srinivasan · M. Pushpavanam (✉)
Central Electrochemical Research Institute,
Karaikudi 630 006 Tamil Nadu, India
e-mail: malathypush@yahoo.com

Table 1 Bath compositions used for Zn–Co alloy depositions

Zn–Co acid		Zn–Co alkaline	
ZnSO ₄ ·6H ₂ O	145 g l ⁻¹	ZnO	9–12 g l ⁻¹
CoSO ₄ ·7H ₂ O	20 g l ⁻¹	NaOH	12–120 g l ⁻¹
H ₃ BO ₃	30 g l ⁻¹	CoSO ₄ ·7H ₂ O	0.8–3 g l ⁻¹
Trisodium citrate	6 g l ⁻¹	TEA	20–25 g l ⁻¹
pH	3–4	pH	13–14

Materials and methods

Preparation of baths

Zn–Ni and Zn–Co alloys were prepared from acid and alkaline electrolytes of the compositions (Tables 1 and 2) mentioned earlier [29–39]. Since alkaline baths cannot yield compact deposits, polyvinyl alcohol was used as an additive. Zinc solution was prepared as a concentrate and given due pretreatments to get rid of the metallic impurities. The zinc electrolyte was treated with 3 g l⁻¹ of zinc dust for nearly 4 h with constant stirring. This treatment displaces impurities like copper and other more noble metals than zinc from the solution. The solution was then filtered and electrolyzed at a current density of 0.3 Adm⁻² with steel cathode and zinc anode for a period of 2 h to remove the other metallic impurities. The solution was filtered and made up to the required volume.

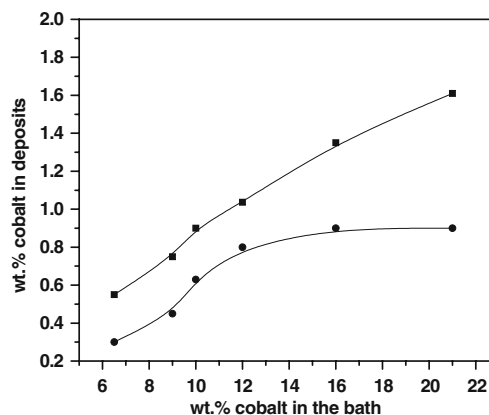
A stock solution of nickel and cobalt were prepared as aqueous solutions for acid baths and as triethanolamine (TEA) complexes for alkaline baths. The required quantity of nickel or cobalt solutions are added to the appropriate quantity of zinc solution and then diluted suitably. The electrolyte's pH was measured with pH meter (Systronix, Model 361) and corrected with dilute sulphuric acid.

Characterisation of deposit's composition

The deposits were analysed for their composition using X-ray fluorescence spectroscopy (CMI, XRX series, USA). The

Table 2 Bath compositions used for Zn–Ni alloy depositions

Zn–Ni acid		Zn–Ni alkaline	
NiSO ₄ ·7H ₂ O	100 g l ⁻¹	ZnO	9–12 g l ⁻¹
ZnSO ₄ ·6H ₂ O	50 g l ⁻¹	NaOH	12–120 g l ⁻¹
NiCl ₂ ·6H ₂ O	40 g l ⁻¹	NiSO ₄ ·7H ₂ O	1–7.5 g l ⁻¹
H ₃ BO ₃	40 g l ⁻¹	TEA	85–120 g l ⁻¹
Trisodium citrate	30 g l ⁻¹	–	–
pH	3–4	pH	13–14

**Fig. 1** Effect of cobalt ratio in solution on its weight percent in deposit: filled square, acid bath; filled circle, alkaline bath

composition and the mass gain obtained during deposition were used to calculate CCE using the formula

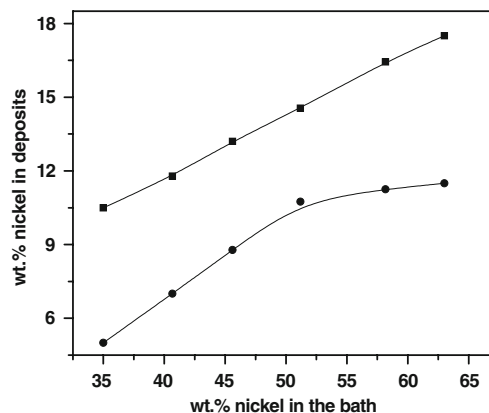
$$\text{Cathode current efficiency (CCE)} = \frac{P_1 W}{Q_1 It} + \frac{P_2 W}{Q_2 It}$$

where P_1 and P_2 are the percentage metal content of zinc and alloying element (cobalt/nickel), respectively, in the deposit, W is the weight of alloy deposited, Q_1 and Q_2 are the electrochemical equivalents of zinc and alloying element (cobalt/nickel), respectively. ' It ' is the total coulombs passed for depositing the alloy.

Morphology and crystallographic characterisation

The structure of the deposits was examined using scanning electron microscope (SEM, Model S3000H, Hitachi, Japan) and the phases analysed using X-ray diffraction (XRD, PANalytical, X'Pert PRO, The Netherlands).

Topography was examined using atomic force microscope (AFM, Molecular Imaging, Scanning probe microscope, model: PICOSPM, USA)

**Fig. 2** Effect of nickel ratio in solution on its weight percent in deposit: filled square, acid bath; filled circle, alkaline bath

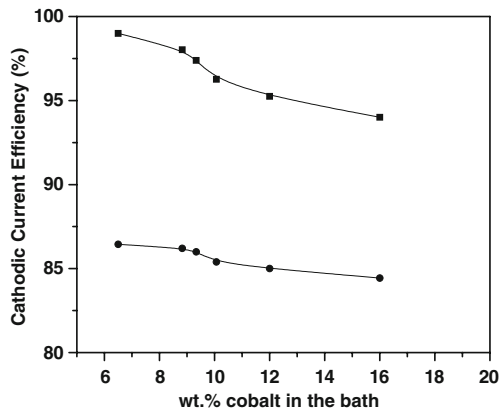


Fig. 3 Effect of cobalt ratio in solution on the CCE of deposition: *filled square*, acid bath; *filled circle*, alkaline bath

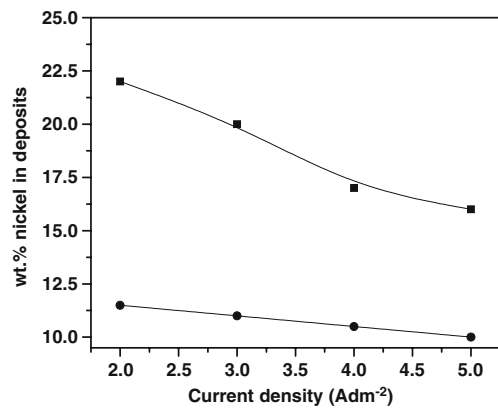


Fig. 6 Effect of current density on the weight percent nickel in deposit: *filled square*, acid bath; *filled circle*, alkaline bath

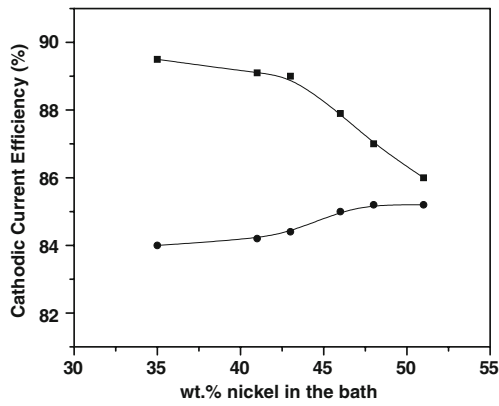


Fig. 4 Effect of nickel ratio in solution on the CCE of deposition: *filled square*, acid bath; *filled circle*, alkaline bath

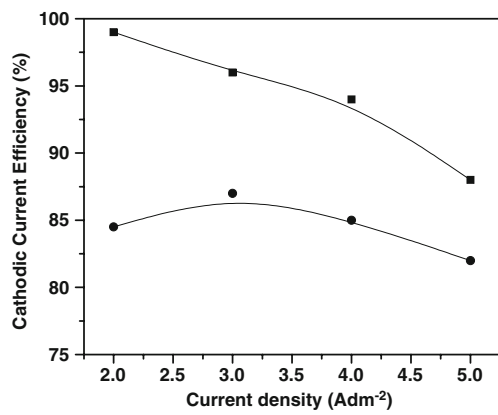


Fig. 7 Effect of current density on the CCE of Zn–Co alloy deposition: *filled square*, acid bath; *filled circle*, alkaline bath

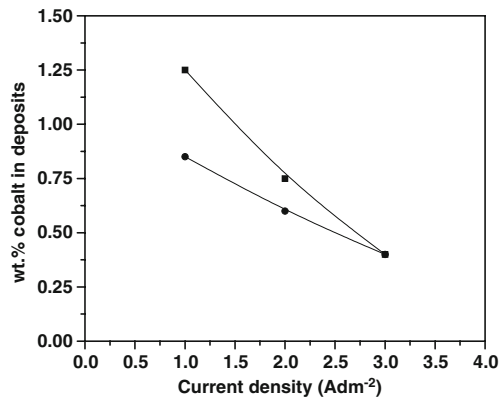


Fig. 5 Effect of current density on the weight percent cobalt in deposit: *filled square*, acid bath; *filled circle*, alkaline bath

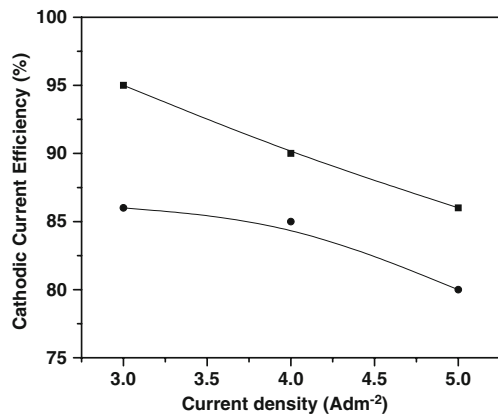


Fig. 8 Effect of current density on the CCE of Zn–Ni alloy deposition: *filled square*, acid bath; *filled circle*, alkaline bath

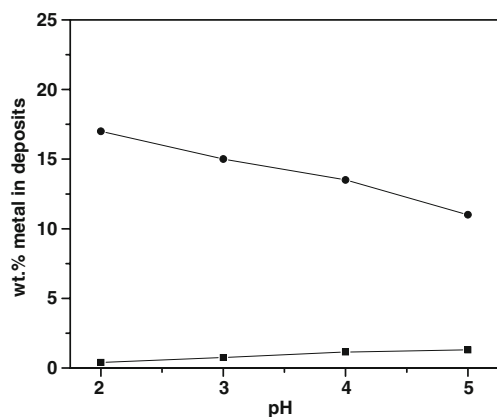


Fig. 9 Effect of solution pH on the Zn–Co/Zn–Ni content of the alloy from acid bath: *filled square*, cobalt; *filled circle*, nickel

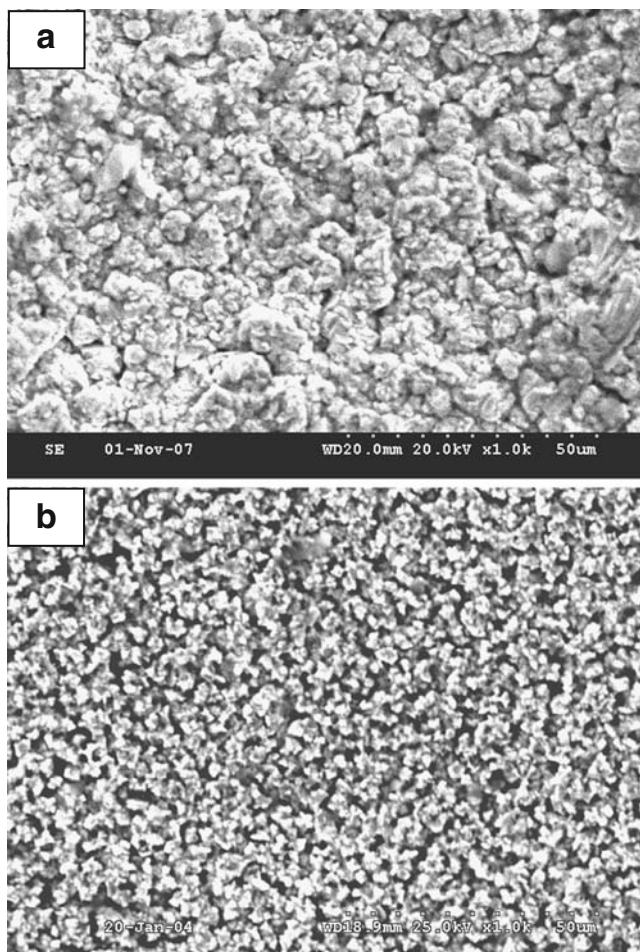


Fig. 10 **a** SEM micrographs of Zn–Co alloy deposit from acid bath. **b** SEM micrographs of Zn–Co alloy deposit from alkaline bath

Corrosion studies

The corrosion resistance of the deposits was confirmed by potentiodynamic polarisation and impedance spectroscopy using Electrochem Analyzer (GillAC, ACM Instruments, serial no.: 1248-Sequencer). A three-necked cell of 250-ml capacity was used. The working electrode was electro-deposited zinc alloy on steel with exposed area of 1 cm^2 with a platinum counter electrode and a saturated calomel reference electrode. Five percent sodium chloride (NaCl) solution was used as the electrolyte. Corrosion tests were conducted at room temperature.

Results and discussion

It is well known that the co-deposition of zinc and cobalt follows the anomalous type in which the less noble metal zinc

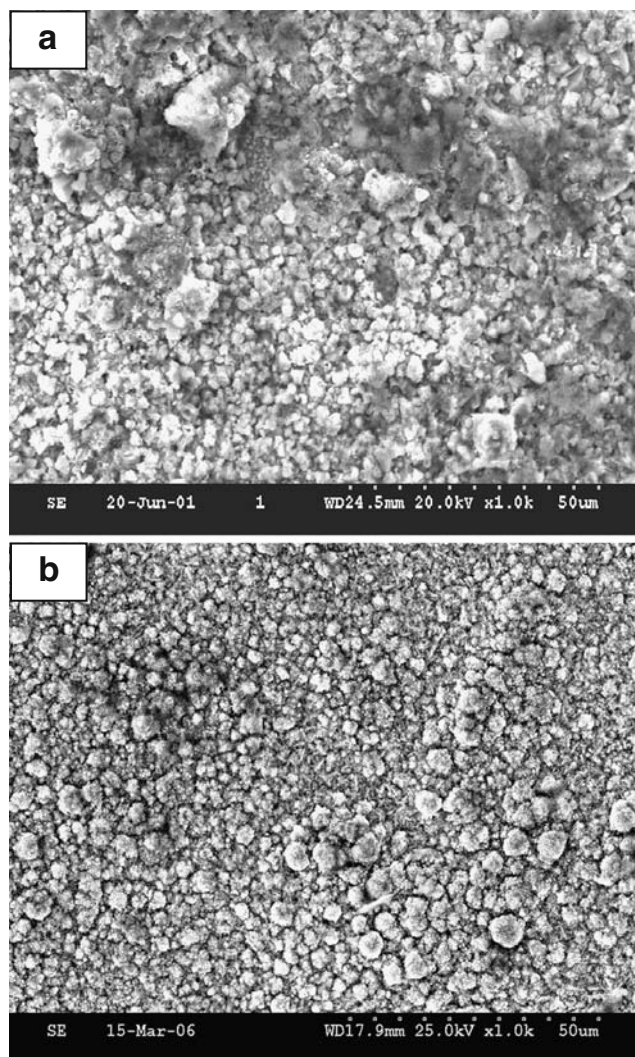
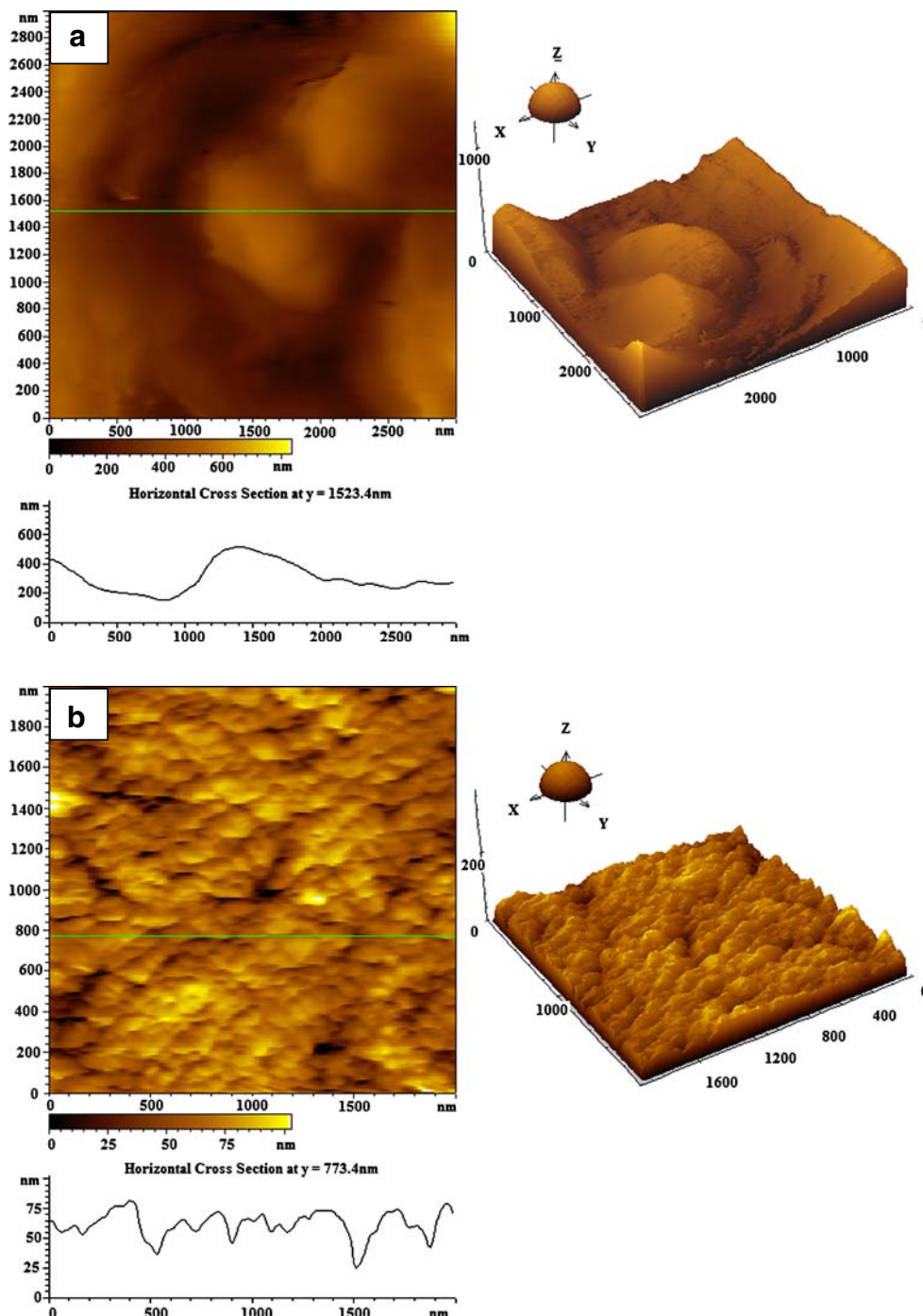


Fig. 11 **a** SEM micrographs of Zn–Ni alloy deposit from acid bath. **b** SEM micrographs of Zn–Ni alloy deposit from alkaline bath

is deposited preferentially [40]. As shown in Figs. 1 and 2, the cobalt or nickel content is always very much on the lower side compared to its metal percent in solution. Figure 1 shows that the cobalt percent in the alkaline bath is considerably less compared to that from the acid bath. Similar behavior is observed in the case of Zn–Ni alloy deposition also (Fig. 2). This is due to the presence of the alloying elements as free ions in acid solutions and as TEA com-

plexes in alkaline solutions. In addition, it is understood that in alkaline baths, the percentage of alloying elements reaches a limiting value above which there is no further increase in spite of the raising of their metal percentage in solution, but the percentage shows a continuously increasing trend in acid baths. The maximum cobalt percent in Zn–Co deposits in acid and alkaline solutions are 0.7–1.6 and 0.4–0.9, respectively, when the metal percent in the solution ranged from

Fig. 12 **a** AFM image of Zn–Co alloy deposit from acid bath showing the grain structure and surface roughness. **b** AFM image of Zn–Co alloy deposit from alkaline bath showing the grain structure and surface roughness

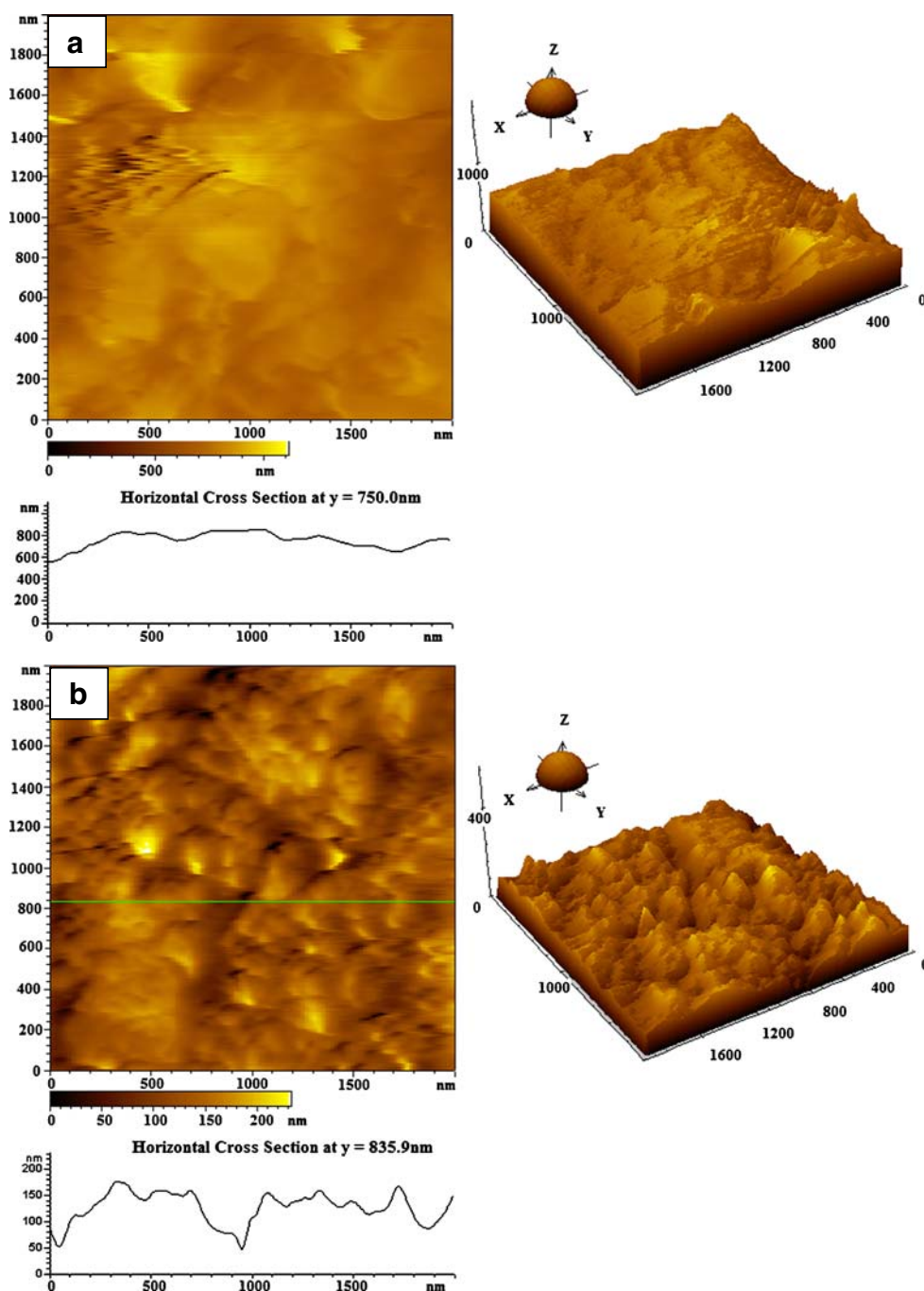


7 to 21. The difficulty in co-deposition of the alloying elements is favourable to obtain deposits with uniform composition even if there is slight difference in their concentration in the solution.

The cathode current efficiencies (in %) of the Zn–Co alloy deposition (Fig. 3) from acid bath ranges from 94 to 99, whereas it is only around 85 in the alkaline baths within the range of metal percent in solution. In Zn–Ni deposition, as shown in Fig. 4, the CCE varies from 90% to 85% in acid

bath and remains at around 85% in alkaline solutions. The lower CCE obtained with the alkaline baths indicate a higher extent of polarisation associated with the deposition. The limited variation in the incorporation of the alloying element indicates their excellent composition dispersion and better throwing power than the acid electrolytes. The acid baths, on the other hand, possess high efficiencies which make the deposits less embrittled with hydrogen, and hence have a high deposition rate [34].

Fig. 13 **a** AFM image of Zn–Ni alloy deposit from acid bath showing the grain structure and surface roughness. **b** AFM image of Zn–Ni alloy deposit from alkaline bath showing the grain structure and surface roughness



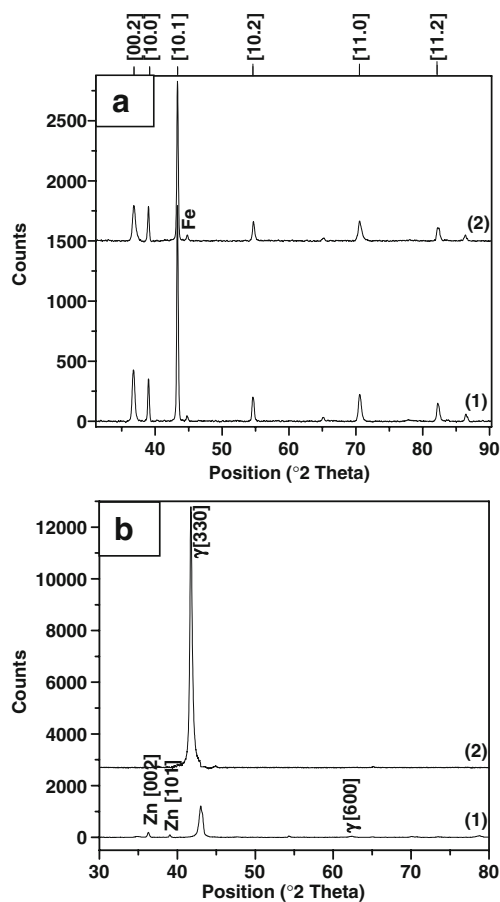


Fig. 14 **a** XRD patterns of Zn–Co alloy deposits from: *1* acid bath, *2* alkaline bath. **b** XRD patterns of Zn–Ni alloy deposits from: *1* acid bath, *2* alkaline bath

Figures 5 and 6 show the effect of current density on the cobalt/nickel content of the deposits. Figures 7 and 8 show the effect of current density on the CCE. Current density has a limiting influence on the percentage incorporation of the metals. This could be understood from the diffusion-limiting

conditions with increasing current density. The cathode efficiency for zinc–cobalt alloy deposition falls from 96 to 88 in acid electrolyte and from 86 to 82 in alkaline electrolyte. In Zn–Ni deposition, the CCE falls from 95 to 85 and from 86 to 80 in acid and alkaline electrolytes, respectively. Loss of current efficiency was related to increased cobalt concentration in the deposit at higher current densities because of activation of the hydrogen-evolution reaction by increased cobalt content. The lower difference in metal percent in the deposit and CCE with increasing current density of the alkaline baths compared to the acid baths accounts for the better current distribution, which is in turn related to the throwing power of these electrolytes.

Figure 9 depicts the effect of pH in both systems under study in acid media. They show a general decrease in nickel and slight increase in cobalt percentage in the alloy. The corresponding CCE of the systems decrease from 87 to 80 and from 96 to 93 for zinc–cobalt and zinc–nickel depositions, respectively, from acid baths.

The photomicrographs of the two alloy systems are shown in Figs. 10 and 11. Zn–Co deposit from an acid electrolyte shows nodular type deposits, whereas that from an alkaline electrolyte is compact and fine-grained in spite of the low metal percentage of cobalt. It has been reported that these systems under suitable conditions and with additives produce nano-grained deposition [38]. Generally, deposits obtained from complex electrolytes yield finer grained deposits because of the higher over-potentials involved, leading to more nucleation than grain growth. In the case of Zn–Ni alloy deposition also, similar trends was obtained, but the effect is less compared to Zn–Co. It is well known that zinc deposits from alkaline non-cyanide baths produce acceptable deposits only in presence of additives [39]. Further improvement in deposit quality and hence the grain structure has been obtained in the presence of additives, as reported by the authors earlier.

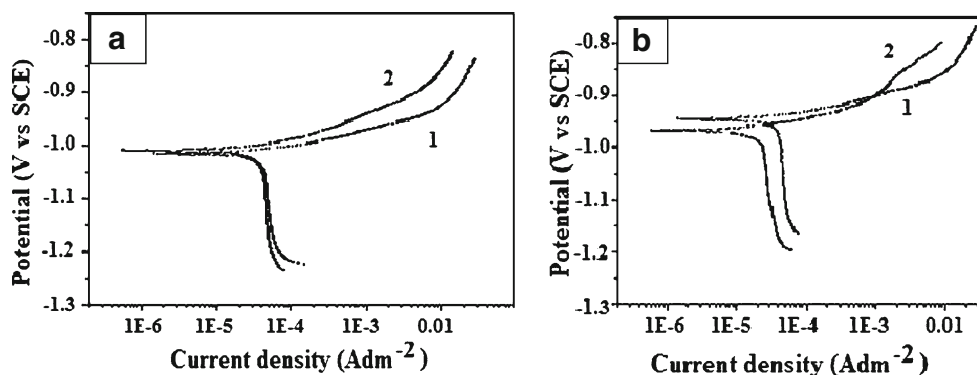


Fig. 15 **a** Potentiodynamic Tafel plot of Zn–Co alloy deposit: *1* acid bath, *2* alkaline bath. **b** Potentiodynamic Tafel plot of Zn–Ni alloy deposit: *1* acid bath, *2* alkaline bath

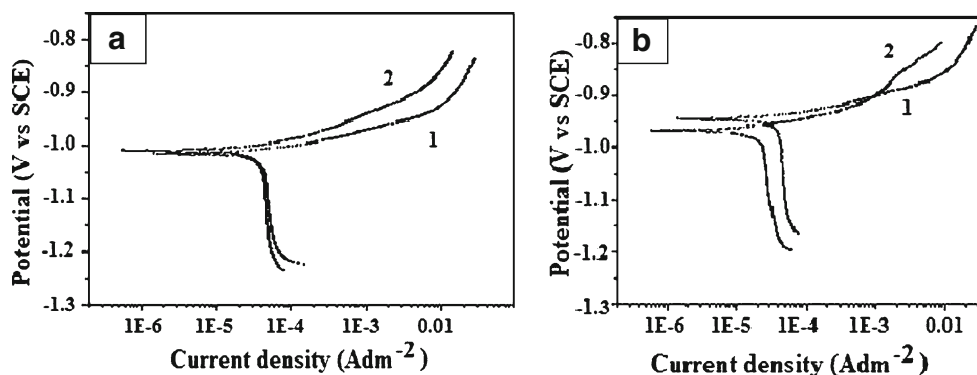


Fig. 16 **a** Nyquist impedance plot of Zn–Co alloy deposit: 1 acid bath, 2 alkaline bath. **b** Nyquist impedance plot of Zn–Ni alloy deposit: 1 acid bath, 2 alkaline bath

AFM figures, given in Figs. 12 and 13, are in support of the above inference. Deposits obtained from acid baths have a much coarser grain size than those obtained from alkaline baths. The roughness values of the deposits from acid baths are of the order of 400–800 nm, whereas for those from alkaline electrolytes, it is in the order of 60–100 nm only.

XRD data given in Fig. 14a,b show that the Zn–Co alloy deposits obtained from the acid and alkaline baths have d values that are similar to pure zinc. It has been reported that below 1 wt% cobalt, the deposit exists only in the η -phase except a slight shift in the 2θ value. The data obtained from both electrolytes are similar, since the cobalt content was maintained almost in the same range. The XRD data for Zn–Ni alloys slightly differ in that the one plated from acid bath shows the existence of γ -phase with a BCC structure and with trace of η -phase of zinc [40], whereas that from the alkaline bath shows relatively high intensity single γ -phase ($\text{Ni}_5\text{Zn}_{21}$) [41–45].

Figures 15 and 16 and Table 3 show the data obtained on corrosion testing. The I_{corr} values of Zn–Co alloys obtained from the alkaline bath is nearly 1.5 times lower than that obtained from the acid bath. The resistance to charge transfer (R_{ct}) values also confirm this behavior. In the case of Zn–Ni, the I_{corr} values are nearly four times lower than those plated from acid electrolytes, and this is supported by the R_{ct} values. The finer grained structure and compact

nature of the deposits from the alkaline baths should have been the reason for this improvement [46].

Conclusions

The acid zinc alloy baths offer higher CCE (rate of deposition) and higher metal co-deposition than the alkaline baths. The latter exhibited better throwing power compared to former. The variation of metal percent in deposit with current density is less significant in alkaline baths, but the variation of CCE with current density is more. The percentage of alloying element for the required application is less in alkaline bath as compared to acid bath. The pH of the electrolyte does not change significantly in alkaline solutions compared to acid solutions. The deposits from alkaline baths are finer grained with a nanostructure than microstructure obtained from acid bath. The corrosion resistance of the deposits from the alkaline baths is higher than that of deposits from acid baths. Overall, the performance of alkaline baths is better compared to acid electrolytes.

Acknowledgment The authors wish to express their sincere thanks to the Director, CECRI for the encouragement given and permission to publish this paper.

Table 3 Data on corrosion resistance obtained from polarisation and impedance techniques

Alloy	Electrolyte	E_{corr} (mV)	I_{corr} (mA cm^{-2})	R_p (Ωcm^2)	R_{ct} ($\times 10^2$; Ωcm^2)	C_{dl} ($\times 10^{-4}$; F)
Zn–Co	Acid	–1005.5	0.0344	14.579	0.92	1.782
	Alkaline	–1010.4	0.02112	28.158	1.15	5.403
Zn–Ni	Acid	–955.86	0.0453	55.777	1.198	2.452
	Alkaline	–998.20	0.0177	75.549	2.192	6.075

References

1. Carpenter EOS, Farr JPG (1998) *Trans Inst Met Finish* 76:135
2. Tsuru T, Kobayashi S, Akiyama T, Fukushima H, Gogia SK, Kammel RJ (1997) *J Appl Electrochem* 27:209
3. Brenner A (1963) *Electrodeposition of alloys—principles and practice*, vol 1. Academic, New York
4. Short NR, Dennis JK, Zhou S (1996) *Surf Coat Technol* 79:218
5. Gabe DR, Green WA (1998) *Surf Coat Technol* 105:195
6. Kalantary MR (1994) *Plat Surf Finish* 81:80
7. Wilcox GD, Gabe DR (1994) *Proceedings of Asian-Pacific Interfinish*, Melbourne-2, Australian IMF, 50.1
8. Crotty D, Griffin R (1997) *Plat Surf Finish* 84:57
9. Short NR, Dennis JK (1997) *Trans Inst Met Finish* 75:47
10. Roper ME, O'Grady J (1996) *Trans Inst Met Finish* 74:3
11. Verberne WMJC (1986) *Trans Inst Met Finish* 64:30
12. Tu ZM, Yang ZL, An MZ, Li WL, Zhang JS (1999) *Trans Inst Met Finish* 77:246
13. Loar GW (1991) *Plat Surf Finish* 78:74
14. Fratesi R, Roventi G, Giuliani G, Tomachuck CR (1997) *J Appl Electrochem* 27:1088
15. Gomez E, Valles E (1997) *J Electroanal Chem* 421:157
16. Kalantary MR, Wilcox GD, Gabe DR (1995) *Electrochim Acta* 40:1609
17. Nabil Z (1999) *Product Finish* 6:53
18. Baldwin KR, Smith CJE (1996) *Trans Inst Metal Finish* 74:202
19. Rajendran S, Bharathi S, Krishna C, Vasudevan T (1997) *Plat Surf Finish* 84:53
20. Carpenter DEOS, Farr JPG (2005) *Proceedings of the 9th International Symposium on Advanced Materials*. Kahuta Research Laboratory, Lahore, Abstracts 101
21. Yan H, Downes J, Boden PJ, Harris SJ (1996) *J Electrochem Soc* 143:1577
22. Carpenter DEOS, Carpenter SD, Farr JPG (2000) *Trans Inst Metal Finish* 78:152
23. Wilcox GD, Mitchell PJ (1987) *Trans Inst Metal Finish* 65:75
24. Gircine O, Ramanauskas P, Castro P, Bertolo-Perez P (2001) *Trans Inst Metal Finish* 79:199
25. Roland P, Gernot S (1996) *Trans Inst Metal Finish* 74:158
26. Pech-Canul MA, Ramanauskas R, Maldonado L (1997) *Electrochim Acta* 42:255
27. Tu ZM, Zhang JS, Li WL, Yang ZL, An MZ (1995) *Trans Inst Metal Finish* 73:48
28. Michael M (1996) PhD thesis, Madurai Kamaraj University, Tamil Nadu, India
29. Pushpavanam M, Natarajan SR, Balakrishnan K, Sharma LR (1991) *J Appl Electrochem* 19:642
30. Pushpavanam M, Raman V, Jayakrishnan S, Shenoy BA (1983) *Metal Finish* 81:85
31. Pushpavanam M, Balakrishnan K (1995) *J Appl Electrochem* 25:283
32. Pushpavanam M, Balakrishnan K (1996) *J Appl Electrochem* 26:1065
33. Pushpavanam M, Balakrishnan K (1996) *Trans Inst Metal Finish* 74:33
34. Siluvai MM, Pushpavanam M, Balakrishnan K (1995) *Br Corros J* 30:317
35. Siluvai MM, Pushpavanam M (2004) *Trans Inst Metal Finish* 82:57
36. Shanmugasigamani, Pushpavanam M (2006) *Trans Inst Metal Finish* 84:326
37. Shanmugasigamani, Pushpavanam M (2008) *Trans Inst Metal Finish* 86:122
38. Dahms H, Croll J (1965) *J Electrochem Soc* 112:771
39. Shanmugasigamani, Pushpavanam M (2005) *J Appl Electrochem* 36:315
40. Beltowska-Lehman E, Ozga P, Swiatek Z, Lupi C (2002) *Cryst Eng* 5:335
41. Gavriła M, Millet JP, Mazille H, Marchandise D, Cuntz JM (2000) *Surf Coat Technol* 123:164
42. Muller C, Sarret M, Benballa M (2002) *J Electroanal Chem* 519:85
43. Ramanauskas R, Gudaviciute L, Kalinichenko A, Juskenas R (2005) *J Solid State Electrochem* 9:900
44. Lee HY, Kim SG (2000) *Surf Coat Technol* 135:69
45. Hall DE (1983) *Plat Surf Finish* 70:59
46. Ramanauskas R (1999) *Appl Surf Sci* 153:53